Effect of Chemically Modified Titanium Surfaces on Protein Adsorption and Osteoblast Precursor Cell Behavior

Jiří Protivínský[1]/Mark Appleford, PhD[2]/Jakob Strnad, PhD[3]/Aleš Helebrant, PhD[4]/Joo L. Ong, PhD[5]

Purpose: To investigate the effects of different chemically modified titanium surfaces on protein adsorption and the osteoblastic differentiation of human embryonic palatal mesenchymal (HEPM) cells. Materials and Methods: Three different surfaces were evaluated. The first, a machined surface (Ti-M), was considered a control. The second surface was acid etched (Ti-AE). The third surface was prepared by exposing the Ti-AE samples to sodium hydroxide (NaOH) solution (Ti-AAE). The surface characteristics of chemically modified titanium were investigated by means of scanning electron microscopy (SEM), Fourier transform infrared spectroscopy (FTIR), and profilometry. To evaluate the production of biomarkers, commercial kits were utilized. Results: Surface composition and morphology affected the kinetics of protein adsorption. Ti-AE surfaces manifested a greater affinity for fibronectin adsorption compared to Ti-M or Ti-AAE surfaces. It was observed that Ti-AE and Ti-AAE surfaces promoted significantly greater cell attachment compared to Ti-M surfaces. Statistically significant differences were also observed in the expression of alkaline phosphatase (ALP) activity, osteocalcin, and osteopontin on all 3 titanium surfaces. ALP activity and osteocalcin production up to day 12 suggested that differentiation of the cells into osteoblasts had occurred and that cells were expressing a bone-forming phenotype. Conclusions: It was thus concluded from this study that surface morphology and composition play a critical role in enhancing HEPM cell proliferation and differentiation into osteoblast cells. (More than 50 references) INT J ORAL MAXILLOFAC IMPLANTS 2007;22:542–550

Key words: cell attachment, cell proliferation, differentiation and mineralization, fibronectin, osteoblast precursor cells, protein adsorption

The morphology of an implant surface, including roughness, has been shown to influence implant fixation in bone and subsequent osteoconduction.[1] Histologic analyses have suggested that bone forms easily on implant surfaces roughened by sand blasting or plasma spraying, whereas fibrous connective tissues have been more frequently observed on smooth machined implant surfaces.[2]

It has been well established that surface roughness, among other surface characteristics, affects cell response. In particular, osteoblastlike cells have been observed to exhibit roughness-dependent phenotypic characteristics, and these cells tend to attach more readily to surfaces with rougher microtopography.[3–8] Moreover, more differentiation of osteoblastlike cells to mature osteoblasts has been reported on roughened implant surfaces compared to smooth implant surfaces.[9]

It has also been reported that a variety of cells orient themselves in the grooves of micromachined surfaces.[10] At the cellular level, biological responses, such as the orientation and migration of cells and cellular production of organized cytoskeletal arrangements, have been reported to be directly influenced by the surface topography.[11] Although it is known that surface roughness is critical to enhance osteoblast responses, the optimal rough-

[1]PhD Candidate, Department of Glass and Ceramics, Institute of Chemical Technology, Prague, Czech Republic; Visiting Research Fellow, Department of Biomedical Engineering, University of Texas at San Antonio, San Antonio, Texas.

[2]Assistant Professor, Department of Biomedical Engineering, University of Texas at San Antonio, San Antonio, Texas.

[3]Chief Scientific Officer, Lasak, Prague, Czech Republic.

[4]Dean and Professor, Department of Glass and Ceramics, Institute of Chemical Technology, Prague, Czech Republic.

[5]Chair and Professor, Department of Biomedical Engineering, University of Texas at San Antonio, San Antonio, Texas.

Correspondence to: Dr J. L. Ong, Biomedical Engineering, University of Texas at San Antonio, One UTSA Circle, San Antonio, TX 78249. E-mail: anson.ong@utsa.edu

ness for the induction of maximum osteoblast response has yet to be determined. To this end, the role of implant surface morphology in organizing cells on an implant surface needs to be investigated.

Numerous implant surface modification techniques have been utilized to influence osteoblast cell responses in vitro and osseointegration in vivo.[12–18] In the field of dental science, sandblasting, acid and alkali treatments, and anodization are surface modification techniques used on commercially available titanium implant surfaces. Although titanium is a biocompatible metal and has been used in medical implants for more than 30 years, the mechanisms and factors governing cell behavior in its presence and in turn its performance in the human body are not yet fully understood. The precise cellular mechanisms underlying the resorption of old bone by osteoclasts and new bone formation by osteoblasts also remain obscure.[19]

It is well known that the processes by which cells become established upon a surface involve initial attachment followed by cellular spreading. Molecules involved in cell adhesion include extracellular matrix (ECM) molecules, transmembrane receptors such as integrins, and intracellular cytoskeletal components.[20] Among the many ECM proteins, such as vitronectin and thrombospondin, fibronectin (FN) is an important protein that may provide some insight on osteoblast cell differentiation, cell-cell interactions, and cell-matrix interactions.[21] The binding of proteins with implant surfaces has been reported to be dependent on the physico-chemical nature of the metallic implant surface.[22] It is also known that the interaction of proteins at the implant surface induces newly formed tissue in vivo.[23] Therefore, the purpose of this study was to evaluate in vitro osteoblast responses to surface morphology produced by 2 different wet chemical treatments and to assess their influence on FN adsorption.

MATERIALS AND METHODS

Titanium Preparation and Characterization

Disk Preparation. Titanium disks 15 mm in diameter and 2 mm thick were fabricated from a bar of commercially pure grade 4 titanium (Lasak, Prague, Czech Republic). Three surfaces were studied: machined (Ti-M), acid-etched (Ti-AE), and acid-alkali etched (Ti-AAE). Ti-M surfaces were prepared by machining the surface with a CNC lathe at a velocity of 600 rpm and shift of 0.03 mm/turn. After machining, the Ti-M samples were ultrasonically degreased in isopropanol, rinsed twice in distilled water for 10 minutes, and air dried at 110°C. Ti-AE surfaces were prepared by sand-

blasting cleaned Ti-M samples with 250-µm-diameter Al_2O_3 particles for 6 seconds at a pressure of 0.8 MPa. The sand-blasted surfaces were degreased in isopropanol and acid-etched in a solution of hydrochloric acid at 40°C. The acid-etched surfaces were then rinsed twice with deionized water, followed by a final cleaning in ethanol using an ultrasonic cleaner for 15 minutes. To prepare the Ti-AAE surfaces, the Ti-AE surfaces were etched with sodium hydroxide (NaOH) solution at 60°C, rinsed twice with deionized water, washed ultrasonically in ethanol for 15 minutes, and air dried at 110°C. All surfaces were autoclaved prior to cell culture experiments. Surface topography is shown in Fig 1.

Characterization of the Titanium Surface. Representative disks from each group were subjected to surface analysis. The surface topography of the disks was evaluated using scanning electron microscopy (SEM-EDS, Jeol XA-733-superprobe, Jeol, Tokyo, Japan), whereas molecular composition of the different titanium surfaces was measured using Fourier transformed infrared (FTIR) spectroscopy (Nicolet 740; Nicolet, Middleton, WI). Surface roughness was measured by profilometry (Taylor Hobson, Leicester, England) with a diamond-tracking stylus. Average surface roughness (R_a) measurements were made at 10 different locations on each sample to obtain an accurate assessment. For the chemically modified samples, measurements were conducted in all directions, whereas on the machined surfaces, measurements were made perpendicular to the machine markings.

Protein Adsorption Kinetics

Adsorption of a model protein, FN, was measured to gain insight into the influence of surface morphology. Human plasma FN (Millipore/Chemicon, Billerica, MA) was obtained in buffered saline at a concentration of 1 mg/mL, sterile filtered and without preservatives. Three hundred microliters of each protein solution (0.5 mg/mL) was loaded onto titanium surfaces in 24 well plates. The study was conducted in a sterile humidified incubator at 37°C over time. Nonadherent proteins were removed, and samples were carefully rinsed twice with saline solution. The removed solution was saved and recorded as total volume.[24] Protein concentration was analyzed using a micro BCA protein assay (Pierce Chemical, Rockford, IL) and measured using a Bio-Rad Benchmark microplate reader (Bio-Rad, Hercules, CA) at 595 nm. Each protein concentration was calibrated using a standard curve. Degree of adsorption was determined by subtracting the residual protein from the initial added protein. Measurements were performed on 5 replicates at each time point.
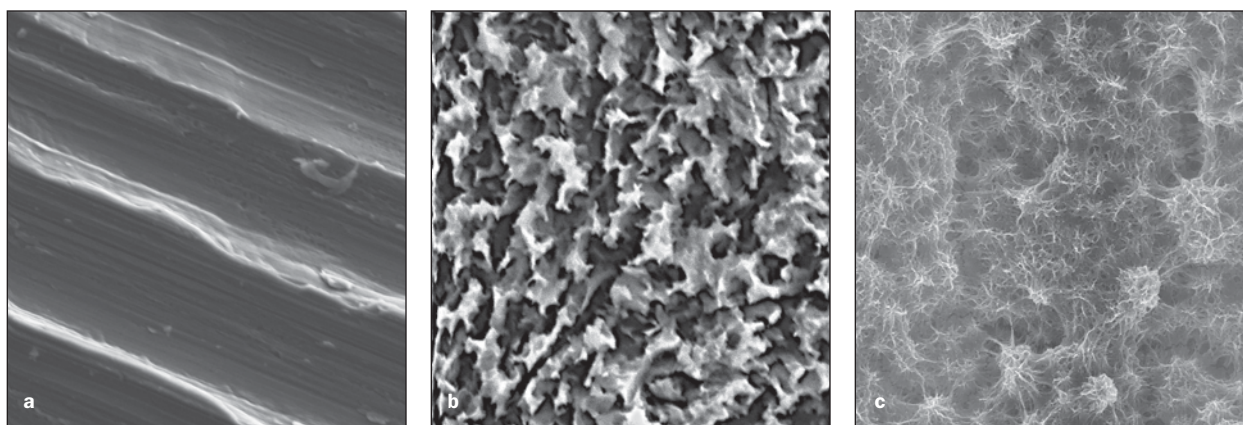
Fig 1 Representative surface topography of *(a)* original machined titanium (Ti-M), *(b)* acid-etched titanium (Ti-AE), and *(c)* alkali-etched titanium (Ti-AAE) surfaces (SEM, original magnification ×4,000).

Cell Seeding and Culture

The osteoblast cell attachment, proliferation, and differentiation assays were performed using ATCC CRL 1486 human embryonic palatal mesenchymal (HEPM) cells, an osteoblast precursor cell line at 37°C in a humidified incubator containing 95% air and 5% CO_2. Dulbecco's modified Eagle's media (DMEM), supplemented with 10% fetal bovine serum, 1% PSA (penicillin 100 units/mL, 100µg/mL streptomycin, and 0.25 µg/mL amphotericin), 10^{-9} mol/L 1.25 (OH)$_2$ vitamin D3, 10 mmol/L B-Glycerophosphate, and 50 µg/mL L-ascorbic acid was used for the cell culture. The culture medium was changed every 3 days with complete DMEM. After 1 week of incubation, the cells were harvested prior to confluence by means of a sterile trypsin-EDTA solution (0.5 g/L trypsin, 0.2 g/L EDTA in normal phosphate buffer saline [PBS], pH 7.4), resuspended in the cell culture medium, and diluted to the desired concentration for each assay.

Cell Attachment. For the cell attachment assay, 300 µL of the osteoblast cell suspension (cell density of 140,556 cells/mL) was seeded on the different titanium surfaces. At selected time intervals (30 minutes, 1 hour, 2 hours, 4 hours, 6 hours), 4 samples from each group were used to determine the number of cells attached. Briefly, samples were removed from the wells and rinsed twice with PBS. The total volume of PBS used for each step was 200 µL. The removed solution was saved, and the total volume was recorded. Cell adhesion was subsequently determined using a Beckman Z2 Coulter Counter (Beckman Coulter, Fullerton, CA). The degree of cell attachment was determined by subtracting the residual cell concentration from the initial cell concentration seeded.

Cell Proliferation. For the cell proliferation assay, the cells were seeded at a cell density of 20,000 cells/cm^2 on different titanium surfaces. At various times after cell seeding (1, 6, 12, 18, and 24 days) pro-liferation was evaluated via quantification of total DNA in each culture. DNA concentration was measured using a PicoGreen assay kit (Molecular Probes, Eugene, OR). Briefly, the cells were washed twice with PBS, lysed using in a 0.2% Triton-X-100 solution, and stored at –20°C until assayed. On the day of the assay, the solution gained from 3 freeze-thaw cycles was brought to room temperature and mixed vigorously for 10 seconds for homogenization. Standards and samples were then added to each well at a volume of 50 µL/well. PicoGreen dye solution was added to each well (150 µL/well) and allowed to incubate for 10 minutes in the dark at room temperature. Fluorescence at 480 nm excitation and 520 nm emission was read on a plate reader to determine DNA concentration per sample. Samples were compared against Lambda DNA standards.

Cell Differentiation. To evaluate cell differentiation, an osteoblast cell density of 20,000 cells/cm^2 was seeded on different titanium surfaces. At various times after cell seeding (1, 6, 12, 18, and 24 days) cell differentiation was evaluated by measuring alkaline phosphatase (ALP) -specific activity, osteocalcin production, and osteopontin production.

To quantitatively analyze ALP activity, the cells were rinsed twice with PBS and subsequently exposed to a 0.2% Triton-X-100 solution to permeate the cell membranes. Cells were then subjected to 3 freeze-thaw cycles, 15 minutes of ultrasonic homogenization, and centrifugation to remove large cellular debris. The resultant supernatant was assayed for the release of p-nitrophenol from p-nitrophenyl phosphate (pH = 10.2), and its specific activity was calculated. Concisely, 50 µL of each sample and standard were pipetted into a 96-well plate, and 50 µL of p-nitrophenyl phosphate substrate was added. The samples were allowed to incubate at room temperature for 1 hour in the dark. The reaction was stopped

with 50 µL of 1 mol/L NaOH, and the absorbance was read at 405 nm using a microplate reader. ALP activity of cells from each surface was calculated from prepared standards (Sigma, St Louis, MO). Results were calculated as nmol p-nitrophenol per hour and normalized to DNA as measured by the PicoGreen assay kit. Data were plotted as the normalized ALP activity at 1, 6, 12, 18, and 24 days.

Production of osteocalcin in this study was measured using a commercially available Mid-Tac Human Osteocalcin EIA Kit (Stougton, MA). On the day of the assay, the samples were thawed at room temperature. The samples (25 µL) or human osteocalcin standard (25 µL) were then added to the microtiter plate provided with the kit. This was followed by the addition of osteocalcin antiserum (100 µL). Incubation was carried out at 37°C for 2.5 hours. The solution was then aspirated, and the plate was washed 3 times with 0.3 mL of PBS. After washing, 100 µL of streptavidin-horseradish peroxidase reagent was added to all wells. After gentle mixing, the solutions were allowed to incubate at room temperature for 30 minutes. The medium was again gently aspirated, and the plate was washed 3 times with 0.3 mL of PBS. One hundred microliters of 3,3', 5,5' tetramethyl-benzidine and hydrogen peroxide solution (1:1 mixture) was then added to all wells and incubated in the dark for 15 minutes. A sulfuric acid solution (100 µL) was added to all wells to stop the reaction. Absorbance was then immediately read at 450 nm using a microplate reader. Osteocalcin concentrations were determined from a standard curve using standards supplied with the kit.

The amount of osteopontin released into the media during culture was measured using an ELISA kit (Assay Designs, Ann Arbor, MI) to determine mid- to late-stage mineralization. Media samples were collected over the culture period and frozen at −20°C until assayed. At the time of assay, the samples were thawed and mixed for 10 seconds. The assay was performed according to the manufacturer's instructions, and absorbance was read at 450 nm, with correction at 550 nm. Samples were compared against human osteopontin standards.

Following the proliferation and differentiation experiment, cells were washed 3 times with PBS solution, then fixed with 2% glutaraldehyde in 0.1 mol/L phosphate buffer. After initial fixation, the specimens were rinsed several times with PBS for 15 minutes, then fixed with 1% osmium tetroxide in 0.1 mol/L phosphate buffer for 1 hour. Samples were then rinsed with PBS for 15 minutes and dehydrated using a series of graded ethyl alcohols (70% for 15 minutes, 95% for 15 minutes, and 3 changes of 100% for 10 minutes each). After dehydration, the specimens were allowed to air-dry overnight. Subsequently, the samples were mounted on aluminum stubs with adhesive tabs and sputter-coated with a thin layer of 60% gold and 40% palladium using a Technics Hummer V sputter coater (Technics, San Jose, CA). Specimens were observed by means of a Philips XL30 environmental scanning electron microscope (FEIC, Peabody, MA).

Statistical Analysis

Statistical analyses were performed using analysis of variance (ANOVA) with Tukey pairwise comparisons, and $P < .05$ was considered necessary for statistical significance. Results are expressed as means ± standard deviations.

RESULTS

## SEM Surface Topography and Roughness

Results of the SEM analysis of the Ti-AE, Ti-AAE, and Ti-M surfaces are shown in Fig 1. Relatively smooth surface features, with parallel and longitudinal both sharp and serrated grooves created by lathe machining were observed for the Ti-M surfaces, whereas round-sharp pits and ridges were observed on acid-etched titanium surfaces. SEM observations revealed hierarchal roughness, with large pits containing small pits, resulting in microporous topography. In contrast to Ti-AE, a porous network structure was formed by the NaOH treatment for the Ti-AAE surfaces. Using profilometry (n = 10), the R_a values for Ti-M, Ti-AE, and Ti-AAE were observed to be 0.81 ± 0.08 µm, 3.14 ± 0.13 µm, and 3.5 ± 0.29 µm, respectively. There was no significant difference in the roughness values of Ti-AE and Ti-AAE surfaces.

FTIR Analysis

Representative FTIR spectrums for Ti-M, Ti-AE, and Ti-AAE surfaces are shown in Fig 2. Analyses of the Ti-AAE surfaces indicated a peak intensity of 1.36 Kubelka-Munk units for the hydroxyl (OH) group at 3384.50 cm^{-1}. A negligible OH peak was observed for the Ti-M and Ti-AE surfaces.

Fibronectin Adsorption Kinetics

The amount of adsorbed FN on different titanium surfaces is seen in Fig 3. A significantly ($P < .05$) greater concentration of FN was adsorbed on Ti-AE and Ti-AAE surfaces over time compared to Ti-M surfaces. FN concentrations on Ti-M surfaces did not significantly change throughout the course of the experiment. Contrary to Ti-M, FN concentrations on Ti-AE and Ti-AAE were observed to be time-dependent. The amount of FN adsorbed on Ti-AAE surfaces
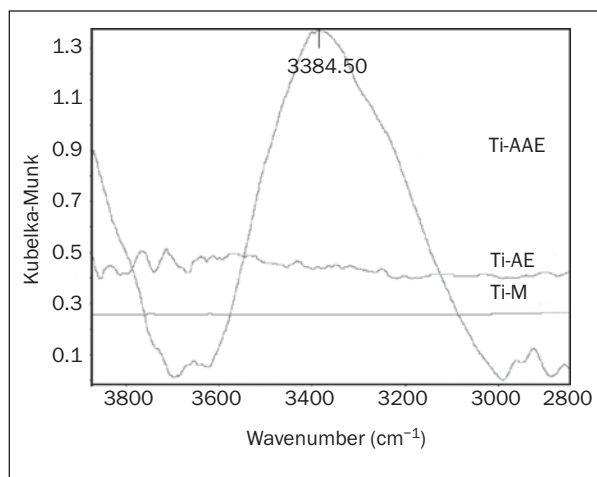
Fig 2 The FTIR spectrum of Ti-M, Ti-AE, and Ti-AAE samples.
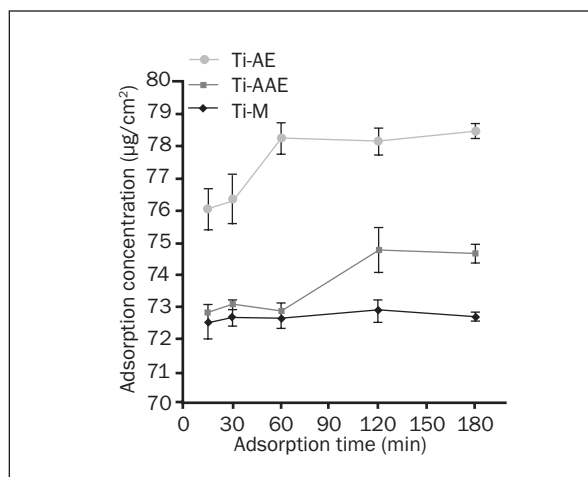
Fig 3 FN adsorption kinetics of 0.5 mg/mL FN over a 3-hour period. Values represent means ± standard deviation (n = 5).
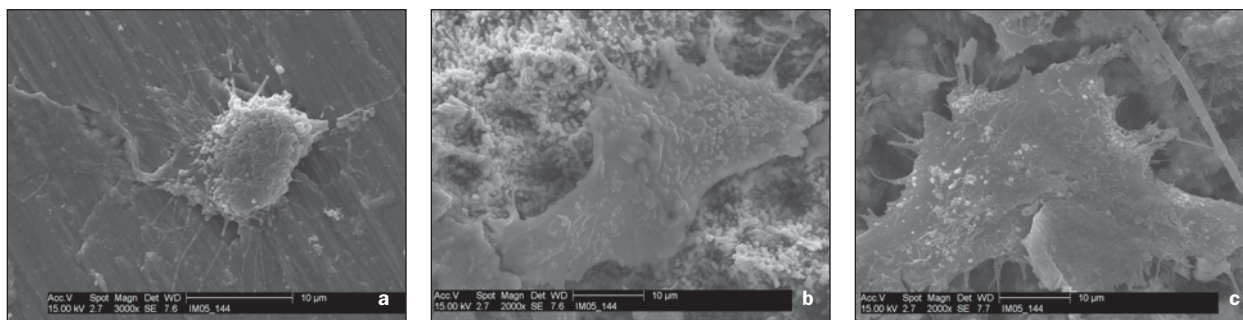
Fig 4 SEM images of osteoblast precursor cells plated on (a) Ti-M, (b) Ti-AE, and (c) Ti-AAE surfaces after 6 hours of cell culture.

was observed to continually increase, and by 60 minutes, a steady state was achieved. The Ti-AE surfaces exhibited a similar adsorption profile, except that there were early and late observed plateaus. A temporary level was observed for the Ti-AE surfaces for the initial FN adsorption for the first 60 minutes, and a second plateau was observed at 120 minutes.

Cell Morphology
Figure 4 shows that the attached cells were highly dissimilar in morphology depending on the surface treatment after 6 hours of incubation. Cells cultured on Ti-M surfaces were observed to possess spindle-shaped features, whereas cells cultured on Ti-AE and Ti-AAE surfaces were observed to spread out, displaying numerous filopodia projecting from the cell body to the titanium surface.
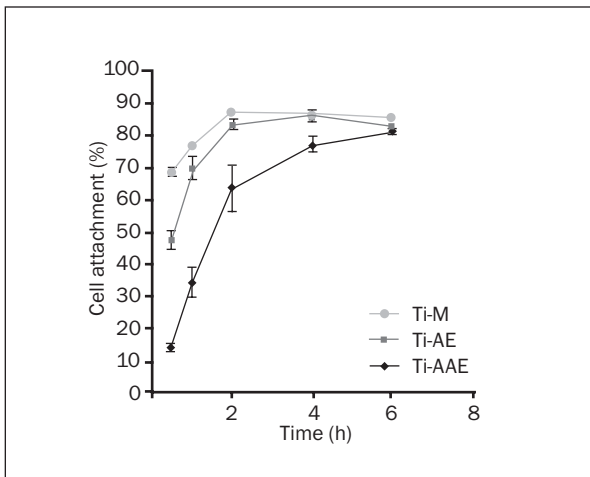
Cell Attachment
As shown in Fig 5, surface morphologies can significantly affect cell attachment at the early stage of cell-material interaction. Cell adhesion to Ti-AAE and Ti-AE demonstrated an initial log-phase adhesion over the first 2 hours incubation, followed by a state

of equilibrium in the second hour. This behavior was maintained over the remaining time points. Equilibrium was defined as the time at which no significant change in percentage of adhesion was observed. Additionally, cells plated on Ti-M surfaces exhibited significantly lower adhesion compared to Ti-AAE and Ti-AE over time.

Cellular Proliferation
During the 24-day experiment, the total cell number, as measured by DNA content, increased by 1 order of magnitude and was observed to follow an exponential growth pattern (Fig 6). Cell proliferation was observed to be similar on all surfaces after 1 day of culture. On day 6, cell proliferation was significantly higher on Ti-AE surfaces compared to Ti-M or Ti-AAE surfaces ($P < .05$). At day 12, no difference in cellular proliferation was observed between the 3 different surfaces. After 12 days of incubation, the number of cells increased sharply. However, no difference in cell proliferation was observed between Ti-M and Ti-AE surfaces after 12 days of incubation. A statistically significant difference in cell proliferation was not observed between any of the substrates after 24 days of culture.

Fig 5 Osteoblast precursor cell attachment on Ti-M, Ti-AE, and Ti-AAE. Values represent means ± standard deviation (n = 5).
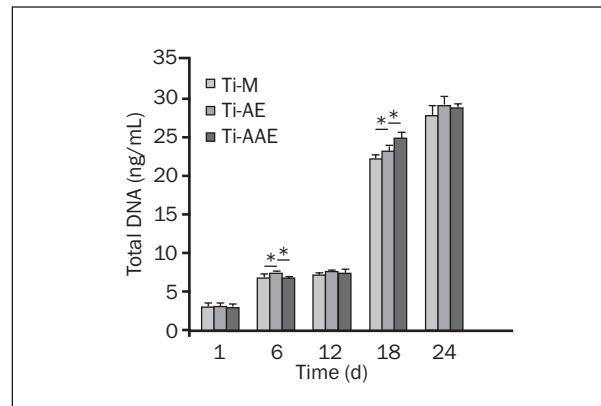
Fig 6 Osteoblast precursor cell proliferation after 1, 6, 12, 18, and 24 days of culture on Ti-M, Ti-AE, and Ti-AAE. Values represent means ± standard deviation; each bar represents 5 disks. * denotes a statistically significant difference ($P < .05$).
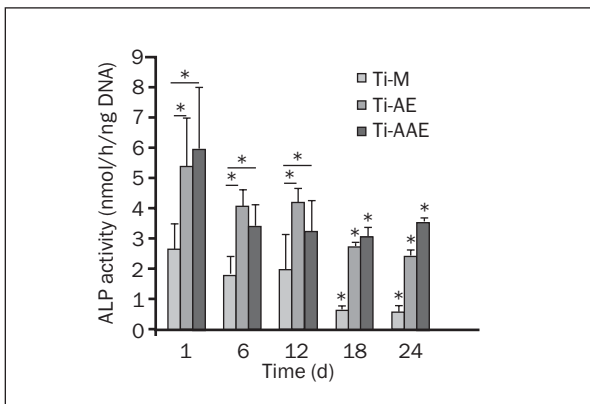
Fig 7 Alkaline phosphatase activity of Ti-M, Ti-AE, and Ti-AAE seeded with osteoblast precursor cells over 24 days. Values represent means ± standard deviation; each bar represents 5 disks. * denotes a statistically significant difference ($P < .05$).
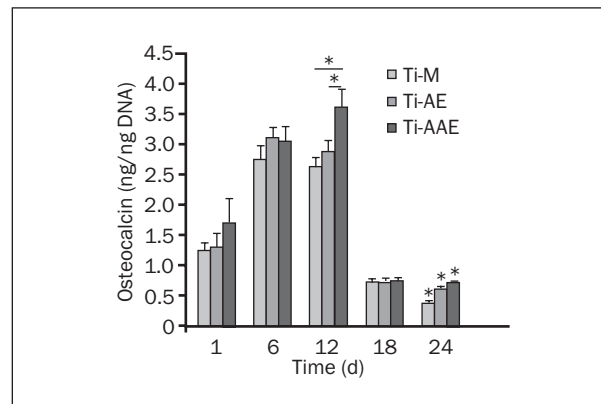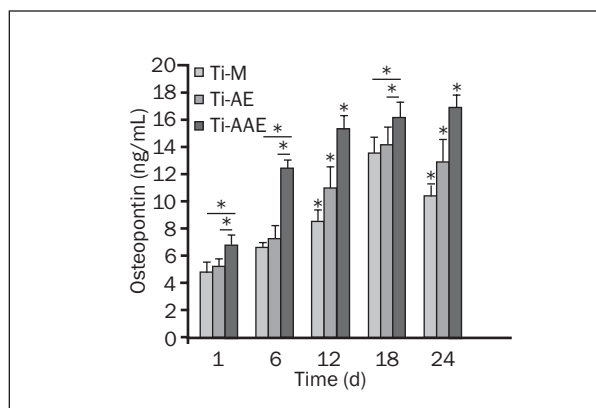

Fig 8 Osteocalcin production after 1, 6, 12, 18, and 24 days of culture on Ti-M, Ti-AE, and Ti-AAE. Values represent means ± standard deviation; each bar represents 5 disks. * denotes a statistically significant difference (P < .05).

Cell Differentiation

Cell differentiation was measured by evaluating the expression of protein markers such as ALP, osteocalcin, and osteopontin. As shown in Fig 7, ALP activity of HEPM cells was significantly higher for Ti-AE and Ti-AAE surfaces compared to Ti-M surfaces at days 1, 6, and 12. However, there was no significant difference in ALP activity between Ti-AE and Ti-AAE surfaces at day 1, 6, and 12. On days 18 and 24, significant differences in ALP activity were observed among all groups. Fig 8 shows an increase in osteocalcin production on all surfaces at days 1, 6, and 12. However, no significant difference in osteocalcin production was observed between the 3 substrates at day 6, and a reduction in osteocalcin production on all surfaces was observed after day 12. It was observed that Ti-AAE surfaces exhibited significantly higher osteocalcin production at days 12 and 24

compared to Ti-M and Ti-AE surfaces. No significant difference in osteocalcin production at days 12 or 24 was observed between the Ti-AE and Ti-M surfaces. As expected, serum levels of osteopontin production on all surfaces demonstrated a low expression level during the early incubation period (Fig 9). Osteopontin production on Ti-M and Ti-AE surfaces was observed to increase linearly until day 18, followed by a decrease in production on these surfaces by day 24. In contrast, osteopontin production on Ti-AAE surfaces continued to increase through all time points tested. Significant differences in osteopontin production were observed between Ti-AAE surfaces and other surfaces on days 1, 6, and 18; however, no differences were observed between the Ti-AE and Ti-M surfaces at these time points. On days 12 and 24, significant differences in osteopontin production were observed for all substrates.

Fig 9 Osteopontin production in cultures of osteoblast precursor cells plated on Ti-M, Ti-AE, and Ti-AAE. Values represent means ± standard deviation; each bar represents 5 disks. * denotes a statistically significant difference ($P < .05$).

DISCUSSION

The aim of this study was to gain a better understanding of the influence of chemically-treated titanium surfaces on cell response and FN adsorption. Development of bone-implant interfaces depends mainly on the interactions of bone matrix and cell behavior with the biomaterial surfaces. It has been shown that cells are greatly affected by surface properties that involve surface texture, roughness, hydrophilicity, composition, and morphology.[25–27] Previous in vitro studies have shown that the combination of roughening treatments (sand blasting, acid etching, and/or alkali etching) could give rise to an implant surface with enhanced ability for rapid osseointegration.[28,29]

Ti-AAE surfaces, which are subjected to sandblasting, acid etching, and subsequent alkali etching, are observed to possess desirable surfaces resulting in reproducible apatite formation in vitro.[30,31] This 3-step surface treatment has also been used with promising results in vivo; a dense hydroxyapatite layer, which is considered a favorable substrate for the attachment and proliferation of human osteoblast cells, was formed on titanium with this surface.[32] It was shown that during the process of peri-implant healing, a calcium phosphate cement line containing noncollagenous proteins formed on the implant's surface before the formation of collagenous matrix.[33,34] In the present study, the responses of preosteoblast cells to different titanium surfaces prepared by chemical wet treatments were investigated.

Zhu et al showed that cell attachment, spreading, and subsequent proliferation are not only substantially related to surface roughness and morphology but are also greatly influenced by chemical composition.[35] Findings from this study were in agreement

with the literature, which revealed that cell attachment and spreading improved remarkably on Ti-AE or Ti-AAE surfaces compared to Ti-M surfaces.[36,37] With Ti-AE (highly hydrophobic) and Ti-AAE (highly hydrophilic) samples having similar surface roughness, a significantly higher cell attachment on Ti-AAE surfaces as compared to Ti-AE surfaces suggests that surface wettability may play a substantial role in cell attachment. Other studies have also indicated favorable cell attachment being closely related to high material surface hydrophilicity.[38] It has previously been shown that surface wettability may have a direct or indirect effect on cell attachment.[35,39] The direct cell attachment mechanism involves physicochemical linkages between cells and surfaces, whereas the indirect approach involves the attraction of proteins such as FN or vitronectin (VN), which are believed to play an important role in governing the interactions of implant surfaces with their adjacent matrix.

It is also believed that interactions between the ECM and cells are crucial for the regulation of cell shape and cellular functions such as migration, proliferation, differentiation, and ultimately survival,[40] and that FN and VN are major components of cell adhesive proteins within the ECM.[41] Since early events during implant placement involve protein adsorption at the host-biomaterial interface,[42] and FN was reported to be one of the earliest cell-binding proteins produced by odontoblasts and osteoblasts,[43] FN was selected as a model protein in the present study. In this study, it was observed that FN was preferentially adsorbed on Ti-AAE and Ti-AE surfaces. Findings from this study are consistent with the results of other researchers.[22,44] Deligianni et al reported that rough substrates bind a greater amount of total protein in comparison to smooth surfaces.[3]

Despite previous studies on in vitro relationships between proliferation and surface roughness, no significant difference in cell proliferation was observed in this study, suggesting that a significant amount of cell growth and division was occurring on all samples investigated.[45,46] In addition, the absence of statistical significance with respect to cell proliferation indicates that all samples evaluated in this study provided a biologically favorable environment.

In contrast, ALP activity in this study was observed to be surface-dependent. ALP activity is regarded as an early marker of bone cell differentiation.[47] Generally, surface roughness is believed to affect cell proliferation and differentiation.[48] In cells cultured on Ti-M surfaces, ALP activity was decreased compared to Ti-AE and Ti-AAE surfaces. It has been shown that titanium roughness generated by acid etching reduces proliferation of bone marrow cells but initially increases the expression of specific cell markers except for ALP.[14]

Other studies have reported the occurrence of elevated ALP activity on NaOH-treated surfaces.[49] Considering the differences in ALP activity of the 2 test materials (Ti-AE and Ti-AAE) and their similar roughnesses, the results cannot simply be attributed to difference in surface roughness. The effects of microtopography and surface chemistry must also be considered.

Osteopontin, another significant glycoprotein characteristic of cell differentiation, was detected on all surfaces at days 1, 6, and 12.[50] Similarly, it was observed that Ti-AAE surfaces had significant effects on differentiation, was of HEPM cells, including enhancement of the expression of osteocalcin. Osteopontin as well as osteocalcin are expressed later during the third period of extracellular-matrix mineralization.[51,52] Osteopontin is expressed early in bone cell differentiation, as well as after mineralization commences,[53] while osteocalcin is generally considered to be an intermediate-late marker of osteoblast differentiation.[54,55] In the present study, HEPM cells cultured on Ti-AAE surfaces demonstrated enhanced expression of osteopontin compared to the other substrata at all time points tested. Osteocalcin and osteopontin have been shown to be closely associated with osteoid production and matrix mineralization, which suggests that Ti-AAE surfaces may hold a greater ability to encourage HEPM cell differentiation into osteoblasts compared to other surfaces tested.

CONCLUSIONS

It was demonstrated in this study that preosteoblast cells vary in their responses to titanium surfaces of different microtopographies and surface compositions. In addition, the study has shown that cell responses vary depending on the amount of OH on titanium surfaces. It can be concluded from this study that Ti-AAE surfaces exhibited greater efficiency in promoting the expression of osteoblastic differentiation markers as compared to Ti-AE and Ti-M surfaces. Consequently, it can be concluded that the Ti-AAE surface may serve as a suitable substratum for enhancing cell differentiation and, in turn, may speed up the process of osseointegration.

ACKNOWLEDGMENTS

REFERENCES

1. Götz HE, Müller M, Emmel A, Holzwarth U, Erben RG, Stangl R. Effect of surface finish on the osseointegration of laser-treated titanium alloy implants. Biomaterials 2004;25:4057–4064.
2. Caulier H, van der Waerden JPCM, Wolke JGC, Kalk W, Naert I, Jansen JA. A histological and histomorphometrical evaluation of the application of screw-designed calciumphosphate (Ca-P)-coated implants in the cancellous maxillary bone of the goat. J Biomed Mater Res 1997;35:19–30.
3. Deligianni DD, Katsala N, Ladas S, Sotiropoulou D, Amedee J, Missirlis YF. Effect of surface roughness of the titanium alloy Ti-6Al-4V on human bone marrow cell response and on protein adsorption. Biomaterials 2001;22:1241–1251.
4. Nishio K, Neo M, Akiyama H, et al. The effect of alkali- and heat-treated titanium and apatite-formed titanium on osteoblastic differentiation of bone marrow cells. J Biomed Mater Res 2000;52:652–661.
5. Borsari V, Giavaresi G, Fini M, et al. Comparative in vitro study on an ultra high roughness and dense titanium coating. Biomaterials 2005;26:4948–4955.
6. Schneider GB, Zaharias R, Seabold D, Keller J, Stanford C. Differentiation of preosteoblasts is affected by implant surface microtopographies. J Biomed Mater Res 2004;69A:462–468.
7. Jayaraman M, Meyer U, Bühner M, Joos U, Wiesmann HP. Influence of titanium surface on attachment of osteoblast-like cells in vitro. Biomaterials 2004;25:625–631.
8. Murphy WL, Hsiong S, Richardson TP, Simmons CA, Mooney DJ. Effect of a bone-like mineral film on phenotype of adult human mesenchymal stem cells in vitro. Biomaterials 2005;26:303–310.
9. Links J, Boyan BD, Blanchard CR, et al. Response of MG 63 osteoblast-like cells to titanium and titanium alloy is dependent on surface roughness and composition. Biomaterials 1998;19:2219–2232.
10. Chehroudi B, McDonnell D, Brunette DM. The effects of micromachined surfaces on formation of bonelike tissue on subcutaneous implants as assessed by radiography and computer image processing. J Biomed Mater Res 1997;34:279–290.
11. Flemming RG, Murphy CJ, Abrams GA, Goodman SL, Nealey PF. Effects of synthetic micro- and nano-structured surfaces on cell behavior. Biomaterials 1999;20:573–588.
12. Spriano S, Bosetti M, Bronzoni M, et al. Surface properties and cell response of low metal ion release Ti-6Al-7Nb alloy after multi-step chemical and thermal treatments. Biomaterials 2005;26:1219–1229.
13. Ong JL, David DL, Carnes L, Bessho K. Evaluation of titanium plasma-sprayed and plasma-sprayed hydroxyapatite implants in vivo. Biomaterials 2004;25:4601–4606.
14. Takeuchi K, Saruwatari L, Nakamura HK, Yang JM, Ogawa T. Enhanced intrinsic biomechanical properties of osteoblastic mineralized tissue on roughened titanium surface. J Biomed Mater Res 2005;72A:296–305.
15. Yang Y, Kim KH, Ong JL. A review on calcium phosphate coatings produced using a sputtering process—An alternative to plasma spraying. Biomaterials 2005;25:327–337.
16. Zinger O, Zhao G, Schwartz Z, et al. Differential regulation of osteoblasts by substrate microstructural features. Biomaterials 2005;26:1837–1847.
17. Göransson A, Jansson E, Tengvall P, Wennerberg A. Bone formation after 4 weeks around blood-plasma-modified titanium implants with varying surface topographies: An in vivo study. Biomaterials 2003;24:197–205.

18. Degasne I, Baslé MF, Demais V, et al. Effect of roughness, fibronectin and vitronectin on attachment, spreading and proliferation of human osteoblast-like cells (Saos-2) on titanium surfaces. Calcif Tissue Int 1999;64:499–507.

19. Mulari MTK, Qu Q, Härkönen PL, Väänänen HK. Osteoblast-like cells complete osteoclastic bone resorption and form new mineralized bone matrix in vitro. Calcif Tissue Int 2004;75:253–261.

20. Clover J, Dodds RA, Gowen M. Integrin subunit expression by human osteoblasts and osteoclasts in situ and in culture. J Cell Sci 1992;103:267–271.

21. Moursi AM, Damsky CH, Lull J, et al. Fibronectin regulates calvarial osteoblast differentiation. J Cell Sci 1996;109:1369–1380.

22. MacDonald DE, Markovic B, Allen M, Somasundraran P, Boskey AL. Surface analysis of human plasma fibronectin adsorbed to commercially pure titanium materials. J Biomed Mater Res 1998;41:120–130.

23. Bierbaum S, Beutner R, Hanke T, Scharnweber D, Hempel U, Worch H. Modification of Ti6Al4V surfaces using collagen I, III, and fibronectin. I. Biochemical and morphological characteristics of the adsorbed matrix. J Biomed Mater Res 2003;67A:421–430.

24. Yang Y, Glover R, Ong JL. Fibronectin adsorption on titanium surfaces and its effect on osteoblast precursor cell attachment. Biomaterials 2003;30:291–297.

25. Harris LG, Patterson LM, Bacon C, Gwynn I, Richards RG. Assessment of the cytocompatibility of different coated titanium surfaces to fibroblasts and osteoblasts. J Biomed Mater Res 2005;73A:12–20.

26. Suh JY, Jang BC, Zhu X, Ong JL, Kim K. Effect of hydrothermally treated anodic oxide films on osteoblast attachment and proliferation. Biomaterials 2003;24:347–355.

27. Li LH, Kong YM, Kim HW, et al. Improved biological performance of Ti implants due to surface modification by micro-arc oxidation. Biomaterials 2004;25:2867–2875.

28. Šimůnek A, Strnad J, Novák J, Strnad Z, Kopecká D, Mounajjed R. STI-Bio titanium implants with bioactive surface design. Clin Oral Implants Res 2001;12:393–421.

29. Šimůnek A, Strnad J, Štěpánek A. Bioactive titanium implants for shorter healing period. Clin Oral Implants Res 2002;13:4.

30. de Andrade MC, Filgueiras MRT, Ogasawara T. Nucleation and growth of hydroxyapatite on the titanium pretreated in NaOH solution: Experiments and thermodynamic explanation. J Biomed Mater Res 1999;46:441–446.

31. Kim HM, Miyaji F, Kokubo T, Nakamura T. Preparation of bioactive titanium and its alloys via simple chemical treatment. J Biomed Mater Res 1996;32:409–417.

32. Yan WQ, Nakamura T, Kobayashi M, Kim HM, Miyaji F, Kokubo T. Bonding of chemically treated titanium implants to bone. J Biomed Mater Res 1997;37:267–275.

33. Davies JE, Baldan N. Scanning electron microscopy of the bone-bioactive implant interface. J Biomed Mater Res 1997;36:429–440.

34. Puleo DA, Nanci A. Understanding and controlling the bone-implant interface. Biomaterials 1999;20:2311–2321.

35. Zhu X, Chen J, Scheideler L, Reichel R, Geis-Gerstorfer J. Effect of topography and composition of titanium surface oxides on osteoblast responses. Biomaterials 2004;25:4087–4130.

36. Sammons RL, Lumbikanonda N, Gross M, Cantzler P. Comparison of osteoblast spreading on microstructured dental implant surfaces and cell behaviour in an explant model of osseointegration. A scanning electron microscopic study. Clin Oral Implants Res 2005;16:657–666.

37. Anselme K, Bigerelle M. Topography effects of pure titanium substrates on human osteoblast long-term adhesion. Acta Biomater 2005;1:211–222.

38. Rupp F, Scheideler, Rehbein D, Axman D, Greis-Gerstorfer J. Roughness induced dynamic changes of wettability of acid etched titanium implant modifications. Biomaterials 2004;25:1429–1438.

39. Damsky CH. Extracelluar matrix-integrin interactions in osteoblast function and tissue remodeling. Bone 1999;25:95–96.

40. Grinnell F, Phan TV. Deposition of fibronectin on material surfaces exposed to plasma: Quantitative and biological studies. J Cell Physiol 1983;116:289–296.

41. Kasemo B. Biological surface science. Surf Sci 2002;500:656–677.

42. Thull R. Physicochemical principles of tissue material interactions. Biomol Eng 2002;19:43–50.

43. Dessau W, Sasse J, Timpl R, Jilek F, Mark von der K. Synthesis and extracellular deposition in chondrocyte cultures. J Cell Biol 1978;79:342–355.

44. Altankov G, Grinnell F, Groth T. Studies on the biocompatibility of materials: Fibroblast reorganization of substratum-bond fibronectin on surfaces varying in wettability. J Biomed Mater Res 1996;30:385–391.

45. Anselme K, Linez P, Bigerelle M, et al. The relative influence of the topography and chemistry of TiAl6V4 surfaces on osteoblastic cell behaviour. Biomaterials 2000;21:1567–1577.

46. Keller JC, Stanford CM, Wightman JP, Draugh RA, Zaharias R. Characterization of titanium implant surfaces. III. J Biomed Mater Res 1994;28:939–946.

47. Gronthos S, Zannettino ACW, Graves SE, Ohta S, Hay SJ, Simmons PJ. Differential cell surface expression of the STRO-1 and alkaline phosphatase antigens on discrete developmental stages in primary cultures of human bone cells. J Bone Miner Res 1999;14:47–56.

48. Boyan BD, Batzer R, Kieswetter K, et al. Titanium surface roughness alters responsivness of MG 63 osteoblast-like cells to 1α 25-(OH)$_2$D$_3$. J Biomed Mater Res 1998;39:77–85.

49. Maitz MF, Poon RWY, Liu XY, Pham TM, Chu PK. Bioactivity of titanium following sodium plasma immersion ion implantation and deposition. Biomaterials 2005;26:5465–5473.

50. Roach HI. Why does bone matrix contain non-collagenous proteins? The possible roles of osteocalcin, osteonectin, osteopontin and bone sialoprotein in bone mineralisation and resorption. Cell Biol Int 1994;18:617–628.

51. Aubin JE. Advances in the osteoblast lineage. Biochem Cell Biol 1998;76:899–910.

52. Boanini E, Torricelli P, Gazzano M, Giardino R, Bigi A. Nanocomposites of hydroxyapatite with aspartic acid and glutamic acid and their interaction with osteoblast-like cells. Biomaterials 2006;27:4428–4433.

53. Robey PG, Boskey AL. The biochemistry of bone. In: Marcus R, Feldman D, Kelsey J (eds). Osteoporosis. San Diego, CA: Academic Press; 1996:95–183.

54. Doherty MJ, Ashton BA, Walsh S, Beresford JN, Grant ME, Canfield AE. Vascular pericytes express osteogenic potential in vitro and in vivo. J Bone Miner Res 1998;13:828–838.

55. Desbois C, Karsenty G. Osteocalcin cluster: Implications for functional studies. J Cell Biochem 1995;57:379–383.